Peer-reviewed version available at *Water* **2019**, *11*, 594; doi:10.3390/w11030594

Article

Predicting rainfall and runoff through satellite soil moisture data and SWAT modelling for a poorly gauged basin in Iran

Majid Fereidoon [1,*], Manfred Koch [2] and Luca Brocca [3]

[1] Dr.-Ing.; majid.fereidoon@gmail.com
[2] Prof. Dr. rer. nat.; kochm@uni-kassel.de
[3] PhD; luca.brocca@irpi.cnr.it
* Correspondence: majid.fereidoon@gmail.com or majid.fereidoon@student.uni-kassel.de; Tel.: (+49-561-804-3408)

Abstract: Hydrological models have been widely used for many purposes in water sector projects, including streamflow prediction and flood risk assessment. Among the input data used in such hydrological models, the spatial-temporal variability of rainfall datasets has a significant role on the final discharge estimation. Therefore, accurate measurements of rainfall are vital. On the other hand, ground-based measurement networks, mainly in developing countries, are either nonexistent or too sparse to capture rainfall accurately. In addition to in-situ rainfall datasets, satellite-derived rainfall products are nowadays available globally with high spatial and temporal resolution. An innovative approach called SM2RAIN that estimates rainfall from soil moisture data has been applied successfully to various regions. In this study, firstly soil moisture content derived from the Advanced Microwave Scanning Radiometer for the Earth observing system (AMSR-E) is used as input into the SM2RAIN algorithm to estimate daily rainfall, SM2R-AMSRE, at different sites in the Karkheh river basin (KRB), southwest Iran. Secondly, the SWAT (Soil and Water Assessment Tool) hydrological model is applied to simulate runoff using both ground-based observed rainfall and SM2R-AMSRE rainfall as input. The results reveal that the SM2R-AMSRE rainfall data are, in most cases, in good agreement with ground-based rainfall, with correlations R ranging between 0.58 and 0.88, though there is some underestimation of the observed rainfall, due to soil moisture saturation, not accounted for in the SM2RAIN equation. The subsequent SM2R-AMSRE- SWAT- simulated monthly runoff reproduces well the observations at the 6 gauging stations (with coefficient of determination, $R^2 > 0.72$), though with slightly worse performances in terms of bias (Bias) and root-mean-square error (RMSE) and, again, some systematic flow underestimation than the SWAT model with ground-based rainfall input. Furthermore, rainfall estimations of two satellite products of the Tropical Rainfall Measuring Mission (TRMM), 3B42 and 3B42RT, are used in the calibrated SWAT-model. The monthly runoff obtained with 3B42- rainfall have $0.39 < R^2 < 0.70$ and are slightly better than those obtained with 3B42RT- rainfall, but not as good as the SM2R-AMSRE- SWAT- simulated runoff above. Therefore, in spite of the afore-mentioned limitations, using SM2R-AMSRE rainfall data in a hydrological model like SWAT, appears to be a viable approach in basins with limited ground-based rainfall data.

Keywords: AMSR-E soil moisture product; SM2RAIN; SWAT hydrological model; Karkheh river basin

1. Introduction

Reliable prediction of runoff in large catchments has been a subject of interest in hydrologic sciences for some time and is significant for sustainable management of water resources, design of water infrastructure and flood risk management [1-3]. Understanding the complex relationships between rainfall and runoff processes is essential to accurately predict the surface runoff [4]. This can be achieved by hydrological modeling that, besides simulating surface runoff, also aids in understanding, predicting, and managing water resources and modeling impacts of climate and land use changes on surface water balance [5].

Distributed/semi-distributed hydrological models, such as the Soil Water Assessment Tool (SWAT) [6], have become very popular tools to simulate runoff, sediment and water quality of agricultural watersheds over the last decades [7]. The SWAT model, which requires numerous input parameters, e.g. soil, land-use, topography, meteorological data, should be calibrated and validated at monitoring stations to reduce the error between measured and predicted outputs, before applying the model for specific analyses or predictions [8,9]. However, the performance of hydrological models in predicting streamflow relies heavily on the quality and spatial distribution of the input rainfall observations [10-12]. Although rain gauges as reference instruments provide accurate measurements of rainfall, because of the variability of rainfall in time and space they do not often provide adequate spatial representation of rainfall, especially, in poorly gauged basins [13].

Using remotely-sensed rainfall products, that nowadays are available at various resolutions (temporal and spatial), and with increased accuracy, is an alternative to the use of rain gauge-observed data. Some recent studies used satellite-derived rainfall in hydrological modeling [14-19]. For instance, Stisen and Sandholt [20] evaluated the performance of five satellite-based rainfall products with different spatial resolutions as input into the MIKE SHE model for runoff simulation of four sub-basins of the Senegal River basin in West Africa. They showed a significant improvement in runoff prediction performance, when the model is recalibrated using bias-corrected satellite rainfall data with rain gauge observations. Thiemig et al. [21] investigated the suitability of satellite-derived rainfall estimates as forcing data for the LISFLOOD hydrological model, applying two different bias-correction methods to correct the bias in the satellite-based rainfall estimates.

Among the satellite-based rainfall predictions, the TRMM Multi-Satellite Precipitation Analysis (TMPA) products [22] are still the most widely used in various research studies and applications [23,24]. For example, Dinku et al. [25] evaluated the TMPA-3B43 rainfall products with nine other satellite-based rainfall through a rain gauge network over Ethiopia. Their results showed that TMPA-3B43 performs very well with a Bias value less than 0.1 and a relative root-mean-square error of about 25% at the monthly time scale.

Another approach, overcoming some of the named deficiencies of classical measurements of rainfall, like rain gauge data, is the recently developed method, called SM2RAIN, proposed by [26], which provides an area-integrated time-accumulated rainfall measurement from soil moisture, SM, data, based on the inversion of the soil water balance equation. Brocca et al. [27] carried out a thorough analysis of the physical consistency of the SM2RAIN algorithm, its hypothesis and performance, by using in situ SM observations as input. However, generally, the temporal and spatial scale of ground SM measurements, especially, in developing countries, is limited and insufficient. Hence, satellite SM observations, which use images retrieved from either passive or active microwave sensors, are recommended, due to their ease of operation, global coverage, and proven accuracy [28]. Nevertheless, the derivation of accurate and reliable soil moisture from satellite remote sensing still represents a challenging task, because of uncertainty due to inexact instrument calibration, errors in the retrieval algorithms, noise in the microwave signal and data transmission failure [29,30].

Nowadays, satellite SM products are available at different spatial and temporal resolution (e.g., [31,32]). Two space-borne satellite missions, such as Soil Moisture and Ocean Salinity (SMOS) mission launched by the European Space Agency (ESA) in 2009 [33] and Soil Moisture Active Passive (SMAP) launched by the National Aeronautics and Space Administration (NASA) in 2015 [34] were placed in orbit and dedicated specifically to measure SM. Advanced Microwave Scanning Radiometer — Earth Observing System (AMSR-E) on board of the NASA's AQUA satellite is one of the most commonly used sensor for SM retrieval over the last years, as it has been available from 2002 to 2011 (e.g., [35,36]). However, because of the rather shallow remotely sensed depth of the bare soil layer for AMSR-E SM (< 1 cm), attenuation of the electromagnetic signal is further increased by dense vegetation, snow-covered and frozen soils [37].

SM estimation based on both active and passive microwave sensors has been evaluated successfully in several studies (e.g., [38-40]). For instance, Rahmani et al. [28] extracted surface SM

Preprints (www.preprints.org) | NOT PEER-REVIEWED | Posted: 31 December 2018 doi:10.20944/preprints201812.0361.v1

Peer-reviewed version available at Water 2019, 11, 594; doi:10.3390/w11030594

from SMOS and the active + passive ESA Climate Change Initiative SM products to investigate the correlation between surface SM products and monthly precipitation and temperature data observations in six different regions of Iran, with the final purpose of drought monitoring. Babaian et al. [41] evaluated the accuracy of different simulated surface soil moisture data (using observed van Genuchten-Mualem hydraulic parameters and those obtained with parametric transfer functions) along with retrieved soil moisture content (using ENVISAT/ASAR active microwave and the inversion algorithm of IEM estimates) in the Zanjanrood River sub-basin, in northwestern Iran. Al-Yaari et al. [42] evaluated two passive (SMOS) and active (ASCAT) satellite microwave products at the global scale with respect to SM simulations from MERRA-Land. They found that ASCAT SM product is prone to larger random errors in Iran.

The objective of this work is twofold. Firstly, we aim to evaluate the accuracy of rainfall estimates obtained from SM2RAIN. For this purpose, the AMSR-E SM product generated by implementing the standard NASA algorithm is used as input into the SM2RAIN algorithm to estimate rainfall, called SM2R-AMSRE from now on, at 10 different sites of the Karkheh river basin (KRB). The lack of in-situ SM measurements in Iran, but the availability of AMSR-E SM data over the modeling time period (2003–2006), are the main reasons for choosing the AMSR-E SM product for this study. In order to apply the SM2RAIN algorithm, the parameters are estimated in a calibration period (1st January 2003 to 31th December 2005) and then the performances are validated in a subsequent independent period (1st January 2006 to 30th September 2006) by comparison with ground-based rainfall observations. The comparison with ground-based rainfall observations is carried out to ensure the same response over time. Moreover, the quality of the SM2RAIN rainfall estimations is evaluated further by comparing them with TRMM-satellite- predicted rainfall of two versions of the 7 TRMM-TMPA-products, daily near-real-time (3B42RT) and research-grade (3B42).

Secondly, we aim to assess the suitability of SM2R-AMSRE as input to the SWAT model for monthly streamflow simulation at 6 gauging stations of the KRB. In the preliminary step, the SWAT model parameters are calibrated using SWAT-CUP [43] in the period 1985-1999, using ground observed climate data as input. Once SWAT is calibrated, it is run again for a different time period (1st January 2003 to 31th September 2006) by considering SM2R-AMSRE, and ground observed rainfall datasets as input. Similarly, the two TMPA- products are employed in the calibrated-SWAT model as well to predict the monthly surface runoff at the same gauging stations. Model performances are assessed by comparing observed and predicted monthly runoff obtained through ground-based, SM2RAIN-estimated and satellite-based rainfall inputs.

2. Materials and Methods

2.1. Study area and data collection

The 50700 km2 – area KRB (Figure 1), mainly characterized by Mediterranean climate conditions, is located in southwest Iran, between 30°58–34°56 N latitude and 46°06–49°10 E longitude. Due to its large area and its topography, ranging from mountains above 3600 m a.s.l. in the northern part to the lowlands in the southern parts, the KRB is characterized by different climate conditions.

Preprints (www.preprints.org) | NOT PEER-REVIEWED | Posted: 31 December 2018 doi:10.20944/preprints201812.0361.v1

Peer-reviewed version available at Water 2019, 11, 594; doi:10.3390/w11030594

Mean annual precipitation ranges from 150 mm in the lower arid plains to 750 mm in the mountainous regions in the northern KRB [44]. The catchment has arid and semi-arid climate and most of the annual water flow (more than 64%) occurs during the months January to May [45].

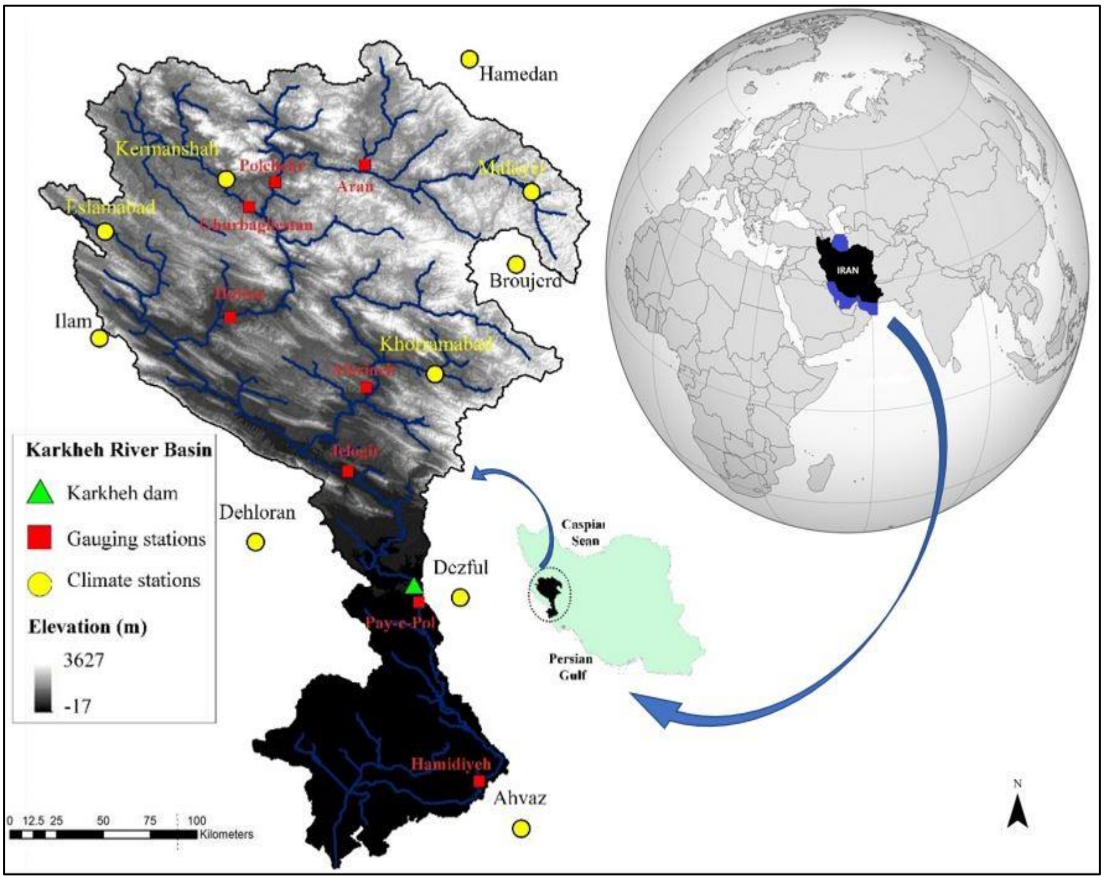

Figure 1. Map of the Karkheh river basin with weather and gauge stations and the Karkheh dam

Geographical characteristics of the gauging and climate stations in the KRB are shown in Table 1. The multipurpose Karkheh reservoir, with a designed storage capacity of 7.5×10^9 m^3 and live storage capacity of 4.7×10^9 m^3 provides water for irrigation of 320,000 ha of agricultural areas in the lower sections of the KRB, as well as generating 934 GWh hydroelectric power per year and controlling flood on the river.

Fereidoon and Koch [46] simulated the long-term monthly discharge in the KRB and found that reservoir regulations have significantly altered the monthly discharge regime in the lower parts of the Karkheh dam, where, among others, streamflow decreased by 50% to 30%. Therefore, as the river flow downstream of the dam is strongly controlled by the reservoir operation rules and, as they are unknown, we excluded the two downstream gauging station in this study and considered only the six remaining gauging stations upstream of the Karkheh dam (see Table 1).

The basic input data used in SWAT model consists of a Digital Elevation Model (DEM) map, provided by Shuttle Radar Topography Mission (SRTM) of NASA at a resolution of 90 m, and a soil map obtained from the global map of the Food and Agriculture Organization of the United Nations (FAO, 1995). Moreover, a 900 m-resolution land-use map is provided by Mahab Ghods Consulting Engineers Co. Daily precipitation, maximum and minimum temperature at 10 meteorological stations are obtained from the Iran Meteorological Organization. In addition, monthly river discharge data from 8 stream gauges are provided by Iranian Ministry of Energy (Figure 1).

The TMPA- 3B42 and TMPA- 3B42RT satellite rainfall products (with 0.250 × 0.250 spatial resolution ≈ 27 km at the Equator) in their latest version 7 used in this study are obtained from (https://pmm.nasa.gov/data-access/downloads/trmm) in daily temporal resolution.

Table 1. Geographical characteristics of the selected gauging (left) and climate (right) stations

Streamgauge Station	Longitude (degrees East)	Latitude (degrees North)	Elevation (masl)	Climate Station	Longitude (degrees East)	Latitude (degrees North)	Elevation (masl)
Aran	47.92	34.42	1440	Hamedan	48.53	34.87	1741
Polchehr	47.43	34.35	1280	Kermanshah	47.15	34.35	1319
Ghurbaghestan	47.25	34.23	1230	Eslamabad	46.47	34.12	1349
Hulian	47.25	33.75	900	Malayer	48.85	34.25	1778
Afarineh	47.89	33.33	820	Broujerd	48.75	33.92	1629
Jelogir	47.80	32.97	350	Ilam	46.43	33.63	1337
Pay-e-Pol[1]	48.15	32.42	90	Khorramabad	48.28	33.43	1148
Hamidiyeh[1]	48.43	31.5	20	Dehloran	47.27	32.68	232
				Dezful	48.38	32.40	143
				Ahvaz	48.67	31.33	22

[1] Stations downstream of the Karkheh dam and not used in this study

2.2. AMSR-E soil moisture product

The Advanced Microwave Scanning Radiometer (AMSR-E) on-board the NASA's Aqua satellite was a passive microwave radiometer, observing brightness temperatures at six different frequencies, ranging from 6.9 to 89.0 GHz. It was launched in May 2002, with a spatial sampling resolution of 25 km, and ceased operations in December 2011. There are several retrieval algorithms available for determining SM products from the AMSR-E data. The daily surface SM product used in this study is based on the NASA algorithm [37,47] and extracted directly from gridded Level-3 land surface product (AE_Land3).

2.3. Hydrological model SWAT and its implementation to KRB basin

The SWAT model is a semi-distributed hydrological model that operates on a daily time-step and was developed in order to assess the impact of water flow, agricultural management practices, sediment and nutrient transport simulation in large complex river basins under different hydrologic, geologic and climatic conditions [6]. SWAT is one of the most widely used hydrological model and has found countless applications all across the world, wherefore more recently the focus has been the simulation of regional hydrological impact of climate change [48-50]. In the SWAT model a catchment or basin is divided into a number of sub-basins (=198 in the present basin), which are then, based on the topography (DEM), soil type, land-use and, optionally, slope characteristics, further subdivided into so-called hydrologic response units (HRUs) with identical characteristic of some of these properties. For the large and complex KRB, the total number of HRU's is more than 11000 (see [46], for details).

For climate input, SWAT uses the data from the weather station closest to the centroid of each subbasin. Calibration, validation and sensitivity analysis of SWAT model are the necessary steps to estimate the meaningful range of many "tuning" parameters of the model. This has historically been done by trial and error but is carried out nowadays more likely by automatic procedure. SWAT-CUP tool, with the SUFI-2 algorithm, which has been used in the current study [43] for model calibration and uncertainty analysis of monthly streamflow. In SUFI-2, the performance of the model is evaluated by two indices: P-factor and R-factor. The P-factor is the fraction of measured data covered by the 95 Percent Prediction Uncertainty (95 PPU) band. Indeed, the propagation of uncertainties in SWAT- parameters leads to uncertainties in the model output variables (surface run off in this study), which are expressed as 95% probability distributions. The 95 PPU is calculated at 2.5% and 97.5% levels of the cumulative distribution of an output variable obtained through Latin hypercube sampling [43]. The R-factor is the average width of the 95 PPU band divided by the standard

Peer-reviewed version available at Water 2019, 11, 594; doi:10.3390/w11030594

deviation of the measured variable. P-factors range between 0 and 1, with values close to 1 indicating a high model performance, while R-factors range between 0 and infinity, with R around 1 to be acceptable for monthly runoff [43]. The quality of the fit of the model output to the observed streamflow data is measured by the root mean square error, RMSE, the determination coefficient, R^2, and the Nash–Sutcliff efficiency, NSE [43].

2.4. SM2RAIN algorithm

The physical processes in the land part of the hydrologic cycle can be mainly described by the soil water balance equation [26]:

$$nZ\, ds(t)/dt = p(t) - q(t) - e(t) - g(t) \tag{1}$$

where n [-] is the soil porosity, Z [L] is the soil layer depth, $s(t)$ [-] is the relative soil moisture, t [T] is the time and p, q, e and g [L/T] are the precipitation, surface runoff, evapotranspiration, and drainage rate (subsurface flow plus deep percolation), respectively. By solving this equation for p and knowing all other variables the rainfall p for each time step can be retrieved from soil moisture data [26, 2014a). Moreover, as shown by [27], the surface runoff q can assume to be negligible.

The drainage rate $g(t)$ is estimated using the following relationship (Famiglietti and Wood, 1994).

$$g(t) = a\, s(t)^b \tag{2}$$

where a [L/T] and b [-] are unknown empirical parameters and are going to be calibrated later. $g(t)$ is the sum of deep percolation and lateral flow.

The (actual) evapotranspiration rate $e(t)$ is represented by a product of the potential evapotranspiration $ET_p(t)$ and the relative soil water content $s(t)$ (e.g., [51]):

$$e(t) = ET_p(t) \times s(t) \tag{3}$$

where $ET_p(t)$ is calculated by means of the theoretical Blaney and Criddle approach as modified by [52]:

$$ET_p(t) = -2 + c[\xi(0.46T_a(t) + 8.13)] \tag{4}$$

where T_a [C⁰] is the mean air temperature, ξ is the fraction of daytime hours for the time step used (daily in this study) in the total daytime hours of the year, and c is a parameter - to be determined in the calibration process further down - that depends on the daytime wind speed, minimum relative humidity and actual insolation time. Although a value of c=1.26 has been proposed for this parameter in many studies (see e.g., [27]), it will be further optimized in the calibration process within an acceptable range (0.8-2.1).

The parameter values nZ, a, b, and c in Equations (2)– (4) are calibrated by matching the SM2RAIN simulated rainfall with the ground observed data in a nonlinear least squares sense, wherefore as objective function, the RMSE is considered, defined as

$$RMSE = \sqrt{\frac{1}{n}\sum_{i=1}^{n}(P_i - O_i)^2} \tag{5}$$

where P_i is the SM2RAIN - predicted daily rainfall (SM2R-AMSRE) and O_i is the daily ground-based observed rainfall at station i. RMSE is minimized by a MATLAB-programed nonlinear constrained optimization method with the named unknown parameters constrained by appropriate bounds.

2.5. SWAT- modeling approach using weather-station- and SM2R-AMSRE precipitation data

Figure 2 shows the flow chart of the various steps to set up and run the SWAT model with ground-based weather station precipitation as well as satellite-based SM2RAIN data. Specifically, after set-up of SWAT streamflow calibration is done by SWAT-CUP using the 1985-1999 gauge-observed rainfall. The calibrated parameter values are considered for further hydrologic simulation

Preprints (www.preprints.org) | NOT PEER-REVIEWED | Posted: 31 December 2018 doi:10.20944/preprints201812.0361.v1
Peer-reviewed version available at Water 2019, 11, 594; doi:10.3390/w11030594

of KRB. After the SM2RAIN algorithm has been applied at the locations of weather stations in the KRB to determine the satellite-based rainfall product, SM2R-AMSR, the latter is then used in the calibrated SWAT-model to predict the monthly runoff between January 2000 and September 2006. The obtained results are then compared with the SWAT output obtained using the in-situ rain gauge observations as input during the same time period.

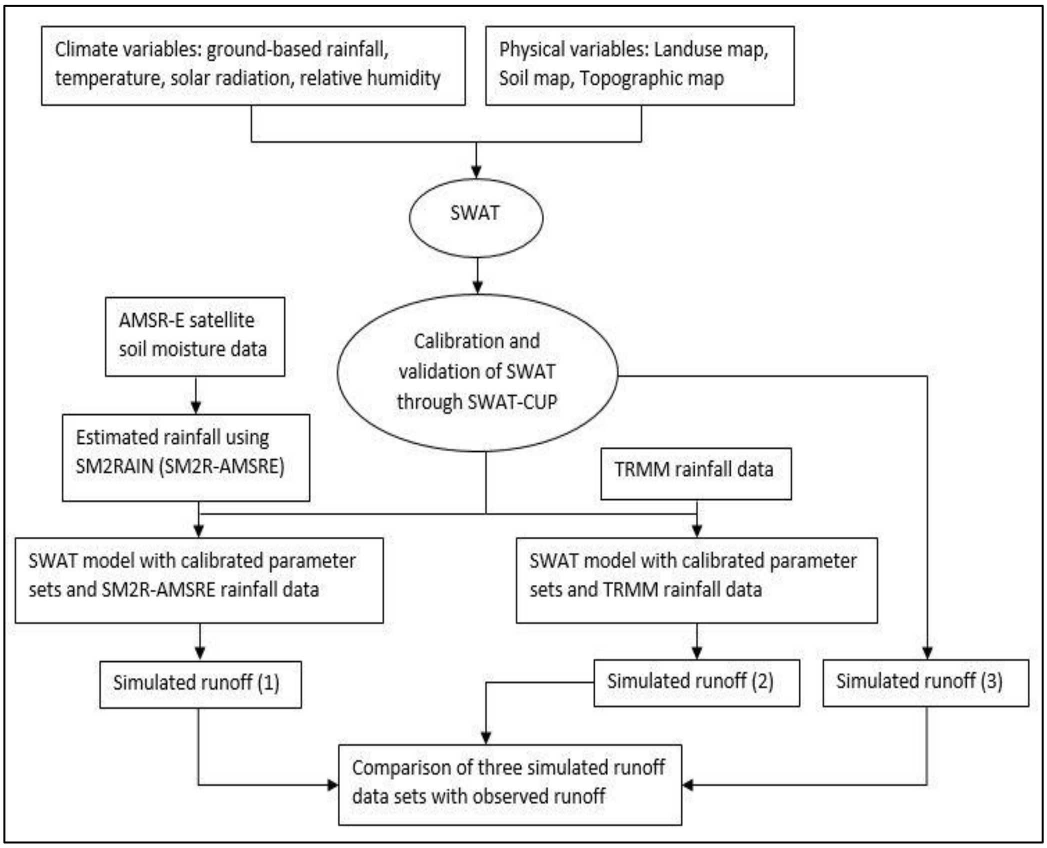

Figure 2. Flowchart for the evaluation of simulated runoff through SWAT using both ground based and SM2R-AMSRE precipitation as input data.

3. Results and Discussion

3.1. SWAT-calibration, validation and sensitivity analysis of streamflow discharge

To evaluate the SWAT model performance for discharge estimation at 6 gauge stations, using ground-based precipitation data, the historical time series from 1985-1999 is considered. Calibration and validation was performed on measured stream flows from 6 gauge stations for the 1985–1995 and 1995–1999 time periods, respectively, wherefore three years (1982–1984) were considered for model warm up. A set of sensitive model parameters is identified in the calibration procedure (see Table 2) in all sub-basins, but with different ranking of sensitivity.

For example, soil and groundwater parameters are found to be most sensitive in lowland catchments, while runoff parameters are the most sensitive ones in mountainous or low mountain range landscapes [53]. This is because under areas with lower slopes, rainfall infiltration accumulates more, leading to higher groundwater levels and, subsequently, to more baseflow contribution to discharge.

Table 2. Initial and final ranges of the 7 most sensitive SWAT calibration parameters in the KRB

Parameter name	Definition	Initial range	Final range

Preprints (www.preprints.org) | NOT PEER-REVIEWED | Posted: 31 December 2018 doi:10.20944/preprints201812.0361.v1

Peer-reviewed version available at Water 2019, 11, 594; doi:10.3390/w11030594

r__CN2	SCS runoff curve number	-0.4 to 0.4	-0.32 to -0.16
v__GWQMN	Threshold depth of water in shallow aquifer required for return flow	1500 to 3500	1520 to 2538
v__ALPHA_BF	Base flow alpha factor	0.4 to 1	0.56 to 0.87
v__EPCO	Plant uptake compensation factor	0.2 to 0.7	0.27 to 0.55
r__SOL_BD	Moist bulk density	0 to 0.35	0 to 0.23
v__RCHRG_DP	Deep aquifer percolation fraction	0.1 to 0.7	0.25 to 0.64
v__SHALLST	Initial depth of water in shallow aquifer	2500 to 4000	2930 to 3849
r__CN2	SCS runoff curve number	-0.4 to 0.4	-0.32 to -0.16

Hence, groundwater parameters, RCHRG_DP, GWQMN, SHALLST and ALPHA_BF, followed by soil parameter SOL_BD are identified to be the more sensitive in the low-elevation (southern) parts of KRB than in the northern part (with higher elevations). It should be noted that the Curve Number at moisture condition II (CN2) is found to be the most sensitive parameter for the watershed as a whole. The performance of the calibrated model is evaluated by four statistical measures, P-factor, R-factor, R^2, NSE at the 6 gauging stations and the results are shown in Table 3 for the calibration and validation periods.

Table 3. Statistical measures for monthly outflows at the 8 gauging stations for calibration and validation periods

Station	P-factor (cal/val)	R-factor (cal/val)	R^2 (cal/val)	NSE (cal/val)
Aran	0.78/0.79	1.12/1.09	0.78/0.79	0.68/0.63
Polchehr	0.81/0.85	1.16/1.11	0.81/0.85	0.72/0.66
Ghurbaghestan	0.89/0.84	1.38/1.03	0.89/0.84	0.68/0.61
Hulian	0.72/0.71	1.05/0.88	0.72/0.71	0.66/0.72
Afarineh	0.94/0.88	1.16/0.89	0.94/0.88	0.73/0.67
Jelogir	0.78/0.75	1.29/0.82	0.78/0.86	0.78/0.74
Pay-e-Pol [1]	0.74/0.70	0.96/0.95	0.73/0.69	0.74/0.68
Hamidiyeh [1]	0.72/0.68	1.31/1.08	0.77/0.76	0.71/0.69

[1] Stations located downstream of the Karkheh dam and not used in this

Figure 3 shows that the SWAT-CUP-simulated monthly streamflow at the 6 gauging stations compares well with the observed data, particularly when considering the 95% uncertainty band.

Peer-reviewed version available at Water 2019, 11, 594; doi:10.3390/w11030594

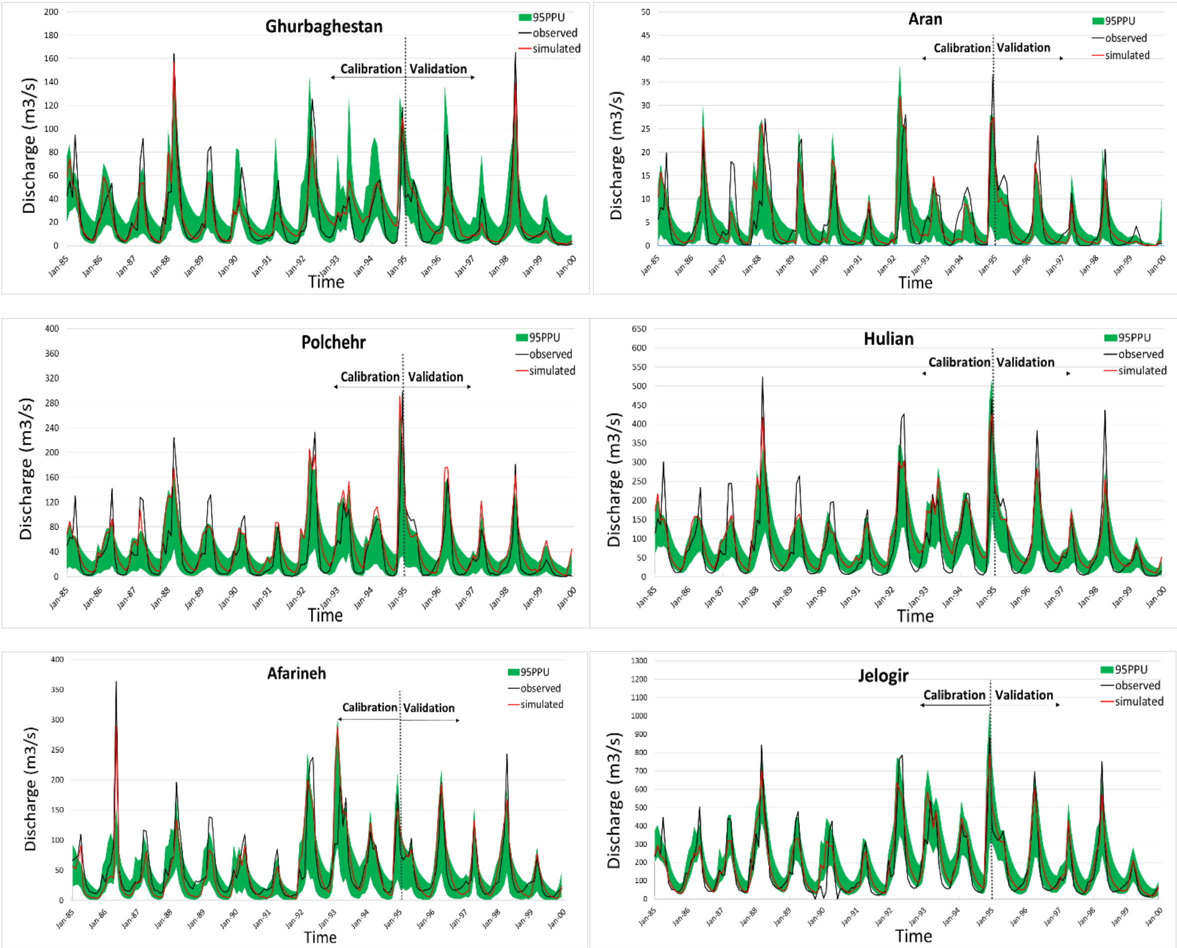

Figure 3. Monthly SWAT calibration/validation of river discharge (1985-1999).

3.2. SM2RAIN- rainfall estimation using AMSR-E soil moisture data

The SM2RAIN method is applied to the locations of the five weather stations in the KRB to estimate the rainfall, called SM2R-AMSRE, from the AMSR-E SM soil moisture data sets. In order to produce a better prediction of the SM2R-AMSRE rainfall, the SM2RAIN- model has to be calibrated first. This is done for the period 1 January 2003 to 31 December 2005; then the model is validated for the remaining 9 months from 1 January 2006 to 30 September 2006.

For evaluating the performance of the SM2RAIN method, the correlation coefficient R, the RMSE (Equation (5)), RRMSE (relative RMSE), and Bias (estimated – observed) are used. As can be seen from Table 4, the SM2RAIN method is able to reproduce the rainfall data from AMSR-E soil moisture products with reasonable accuracy.

Table 4. Statistical measures of the performance of the SM2RAIN algorithm at the different climate stations

Climate Station	**R [-]**		**RMSE [mm]**		**RRMSE [-]**		**Bias [%]**	
	Cal	Val	Cal	Val	Cal	Val	Cal	Val
Ahvaz	0.75	0.66	2.52	2.48	4.04	4.51	-1.05	-1.77
Kermanshah	0.69	0.47	3.07	3.91	2.77	3.66	-3.16	-0.18
Hamedan	0.61	0.54	3.06	2.73	3.05	3.97	-2.57	-0.07
Khorramabad	0.58	0.57	4.19	4.32	3.36	3.16	-4.07	-3.92
Ilam	0.64	0.88	5.58	4.77	3.23	3.65	-6.13	-5.79

In the validation period, the R-values for all five sites range between 0.57 for Khorramabad to 0.88 for Ilam. The RMSE shows the lowest values at Ahvaz station, in accordance with the better R-

Preprints (www.preprints.org) | NOT PEER-REVIEWED | Posted: 31 December 2018 doi:10.20944/preprints201812.0361.v1

Peer-reviewed version available at *Water* **2019**, *11*, 594; doi:10.3390/w11030594

values there. On the other hand, this station has the highest RRMSE, owing to the fact that its average rainfall is the lowest. The Bias estimates range from -1.05 to -6.13 for stations Ahavz and Ilam, respectively. The negative values of Bias at all stations indicates a typical underestimation of the SM2R-MSRE rainfall, for reasons discussed below.

Figure 4 shows both the daily observed and estimated SM2R-AMSRE rainfall, along with the AMSR-E SM time series, for the five climate stations. Obviously, the highest and lowest performance is obtained for stations Ahvaz and Khorramabad, respectively. In general, one can notice from the figure that the SM2RAIN algorithm underestimates the total rainfall amount at all sites. Indeed, at saturation level the SM value remains constant for any rainfall amount; i.e. the SM measurement cannot provide useful information for rainfall estimation. Based on these considerations and the obtained results, it is expected that soil moisture-based methods will provide an underestimation of the total rainfall [26,27,54], due to the saturation of the soil moisture level.

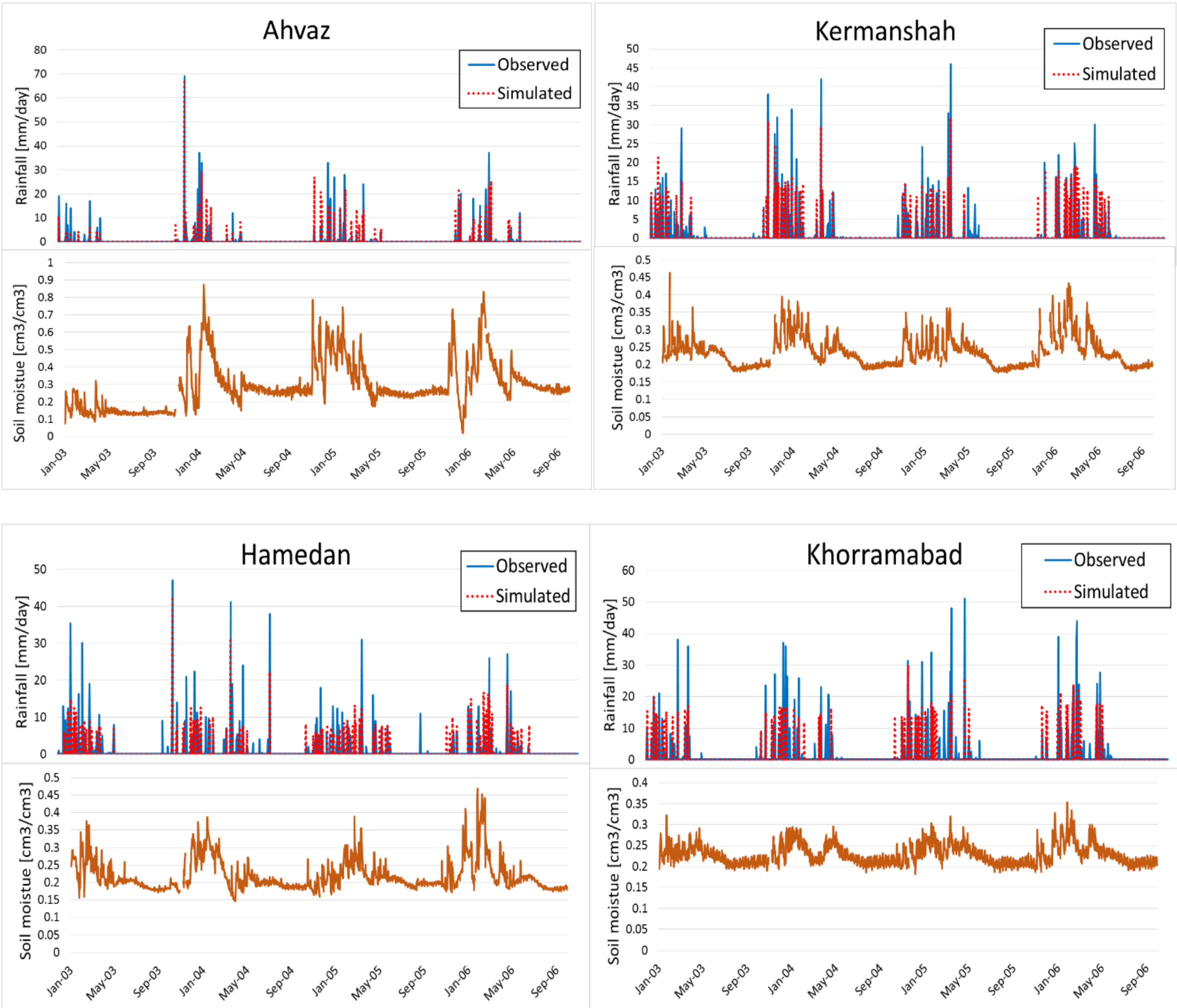

Preprints (www.preprints.org) | NOT PEER-REVIEWED | Posted: 31 December 2018 doi:10.20944/preprints201812.0361.v1

Peer-reviewed version available at Water 2019, 11, 594; doi:10.3390/w11030594

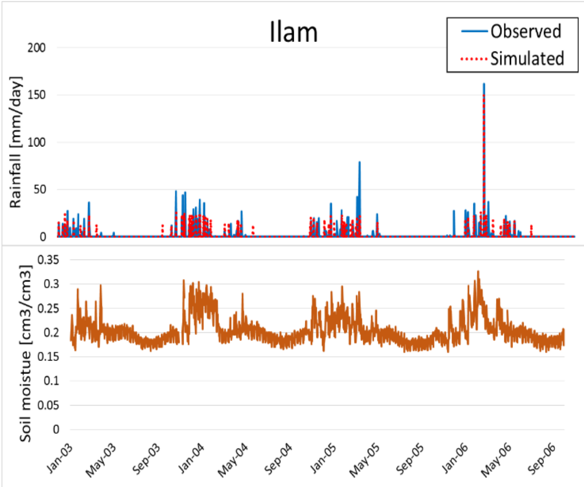

Figure 4. Observed and SM2R-AMSRE- estimated daily rainfall (upper panels) and AMSR-E soil moisture data (lower panels) from January 2003 to October 2006.

As can be seen further in Figure 4, the AMSR-E SM time series at Ilam and Khorramabad stations have higher noise than those at other stations. This could be the reason for the lower performance of the SM2RAIN model at these stations. Moreover, the surface condition may also affect the performance, so that the stations located in mountainous areas, like Ilam and Khorramabad, owing to the occurrence of frozen soils and snow cover, have lower performances than those located at low altitudes, e.g. Ahvaz. In general, the stations located in drier areas, with lower rainfall amounts, like Ahvaz, show better performance, corroborating the saturation statement above. Similarly, high RRMSE- values and more negative of Bias- values at all stations for both calibration and validation periods can be explained by the underestimated SM2R-AMSRE for heavy rainfall events, owing most likely to the earlier-mentioned problem of soil moisture saturation in the SM2RAIN- model.

The four parameter values (see Equations (1)– (3)) found by nonlinear optimization during the calibration of the SM2RAIN models are shown in Table 5. Similar to previous studies (e.g. [26,27]), these parameter values are consistent with their expected physical values.

Table 5. Optimized parameter values of the SM2RAIN equations (1-3) at the various climate stations.

Climate Station	Zn [mm]	a [mm/d]	b	c
Ahvaz	32.1	39	2.2	1.90
Kermanshah	34.8	50	2.3	2.00
Hamedan	58.3	56	1.5	1.20
Khorramabad	32.9	46	1.9	1.95
Ilam	44.6	87	2.5	1.90

The spatial distributions (drawn using the nearest-neighbor interpolation procedure for the rainfall in SWAT) of the rain-gauge-measured- and the SM2R-AMSRE estimated mean annual rainfall over the KRB for the January 2003 to September 2006 time period are shown in the two panels of Figure 5. As can be seen, the SM2RAIN method predicts the ground-based observed rainfall in an agreeable manner, though the latter is slightly underestimated in some regions, for the reasons discussed above.

Preprints (www.preprints.org) | NOT PEER-REVIEWED | Posted: 31 December 2018 doi:10.20944/preprints201812.0361.v1
Peer-reviewed version available at Water 2019, 11, 594; doi:10.3390/w11030594

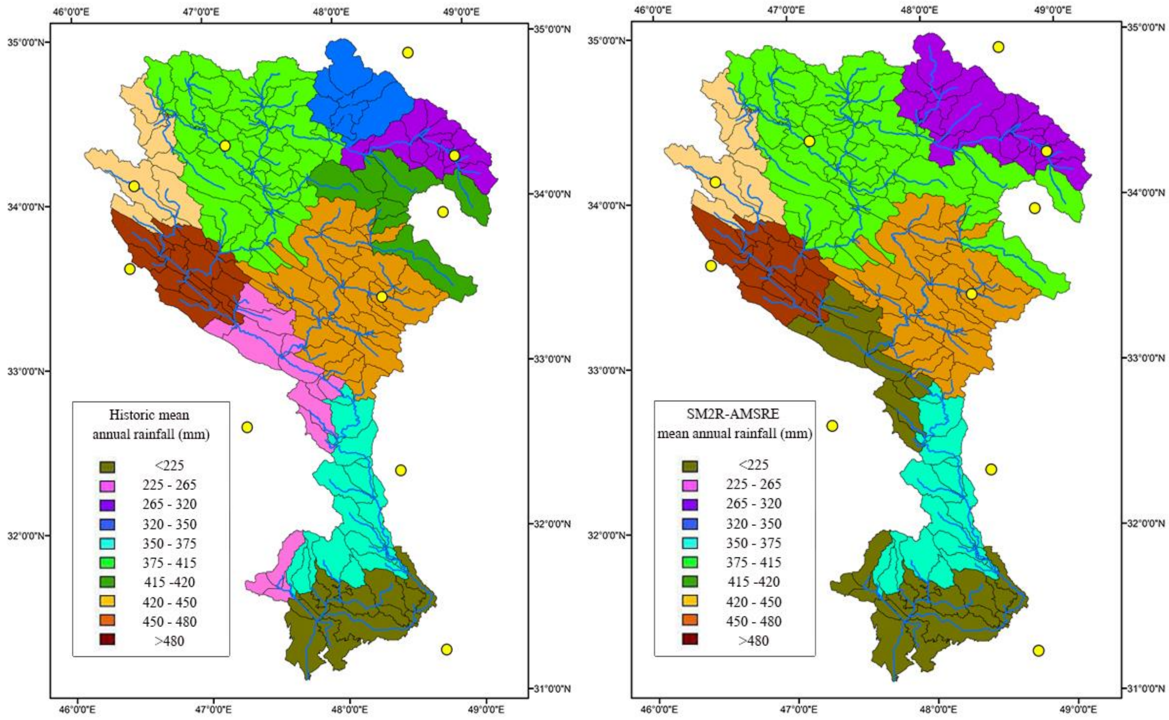

Figure 5. Spatial distributions of rain-gauge-measured (left panel) and SM2R-AMSRE- estimated mean annual rainfall over the KRB for January 2003 to September 2006.

3.3. Contributions of different hydrological components to the SM2RAIN water balance equation

With the purpose of quantifying the contribution of each component of hydrological balance equation (Eqation (1)), i.e. soil moisture change, drainage and evapotranspiration, to the rainfall estimation, calibrated parameter values of the SM2RAIN algorithm are considered for SM2RAIN-AMSRE rainfall simulation. To study in more details, two months, the wet month January 2003, and the dry month July 2004, for stations Kermanshah and Hamedan, respectively, are selected to assess the contribution of the different components to the SM2R-AMSRE rainfall. The results are shown in the corresponding two plots of Figure 6.

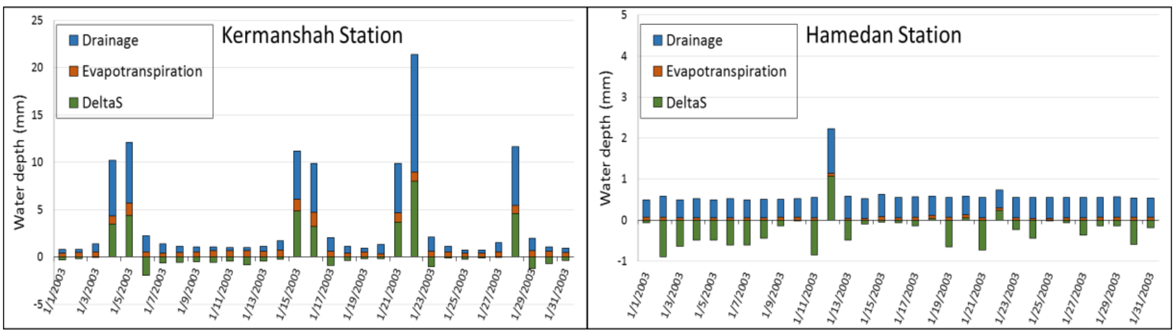

Figure 6. Contributions of the different components of the water balance equation to SM2R-AMSRE at Kermanshah station for January 2003 (left) and Hamedan station for July 2004 (right).

As can be seen drainage and evapotranspiration contribute the most and least to the SM2R-AMSRE during rainfall, respectively. At both stations, similar to the results obtained by [27], the evapotranspiration has a small contribution to SM2R-AMSRE, through SM2RAIN approach. This contribution is even smaller in dry months when the soil moisture content is very low.

Preprints (www.preprints.org) | NOT PEER-REVIEWED | Posted: 31 December 2018 doi:10.20944/preprints201812.0361.v1

Peer-reviewed version available at Water 2019, 11, 594; doi:10.3390/w11030594

3.4. Evaluation of TRMM satellite precipitation products (TMPA)

As a third approach of rainfall estimation, the TRMM (TMPA) satellite products, 3B42 and 3B42RT, are evaluated over the KRB by comparing them with the ground-based measurements. The results are listed in Table 6 in terms of the four statistical scores, R, RMSE, RRMSE and Bias. As can be seen from the table, the 3B42 rainfall products provide better performance in terms of R and Bias, while RMSE and RRMSE are slightly lower for 3B42RT than for 3B42.

Moreover, the comparison of the four statistical measures of the TMPA products (Table 6) with those of SM2R-AMSR (Table 4) indicates that SM2RAIN predicts the observed rainfall consistently more accurately than TMPA, except for the bias at Ahvaz station, which is only 0.23% for TMPA-3B42.

Table 6. Statistical measures of the performance of the TRMM (TMPA3B42, 3B42RT) at the different climate stations

Climate Station	R [-]		RMSE [mm]		RRMSE [-]		Bias [%]	
	3B42	3B42RT	3B42	3B42RT	3B42	3B42RT	3B42	3B42RT
Ahvaz	0.22	0.28	5.04	4.20	8.30	6.91	0.23	6.71
Kermanshah	0.50	0.38	5.09	4.87	4.62	4.43	-35	-9.64
Hamedan	0.46	0.34	3.94	4.09	4.18	4.34	9.62	33.78
Khorramabad	0.75	0.39	6.61	5.77	5.12	4.47	-36.4	15.16
Ilam	0.44	0.29	6.95	7.26	4.25	4.44	-6.1	42.43

3.5. SWAT- predicted runoff driven by ground-based-, SM2R-AMSRE- and TMPA- rainfall

Finally, the January 2003 to September 2006 simulated monthly runoff obtained by using (1) ground-based, (2) the SM2R-AMSRE satellite-based rainfall, and the two TRIMM-TMPA products (3) (3B42 and (4) (B42RT), as input in the calibrated- SWAT model are compared to each other (Figure 7, Tables 7 and 8). For cases (1) and (2), good SWAT- performances, as indicated by the standard statistical measures in Table 7, are obtained. Thus, the R^2-values for all sites are greater than 0.89 and 0.72, when using ground-based- and SM2R-AMSRE rainfall as SWAT- input, respectively.

Table 7. Performance measures for SWAT-predicted runoff using ground-based- and SM2R-AMSRE rainfall.

Station	Ground-based rainfall					SM2R-AMSRE rainfall				
	R^2	RMSE (m^3/s)	RRMSE	NSE	Bias	R^2	RMSE (m^3/s)	RRMSE	NSE	Bias
Aran	0.72	3.08	2.22	0.60	0.86	0.83	2.17	3.18	0.79	1.26
Polchehr	0.82	18.5	14.8	0.70	5.31	0.85	10.1	13.8	0.81	10.2
Ghurbaghestan	0.71	15.5	10.1	0.57	2.65	0.81	7.72	5.27	0.81	8.29
Hulian	0.87	33.6	27.3	0.76	13.9	0.89	18.7	19.6	0.84	19.8
Afarineh	0.82	19.2	14.5	0.56	10.3	0.88	12.2	11.8	0.75	13.8
Jelogir	0.83	50.1	58.6	0.74	13.8	0.87	38.6	45.1	0.92	46.3

The best results in terms of R^2 and NSE are obtained for Hulian gauge station. As expected, due to the already noted systematic underestimation of the SM2R-AMSRE rainfall (see Figure 4), the SWAT model using ground-based observed rainfall shows slightly better performance than that using SM2R-AMSRE data. This underestimation is particularly noticeable at the stream peak flows shown in Figure 7.

Preprints (www.preprints.org) | NOT PEER-REVIEWED | Posted: 31 December 2018 doi:10.20944/preprints201812.0361.v1

Peer-reviewed version available at Water 2019, 11, 594; doi:10.3390/w11030594

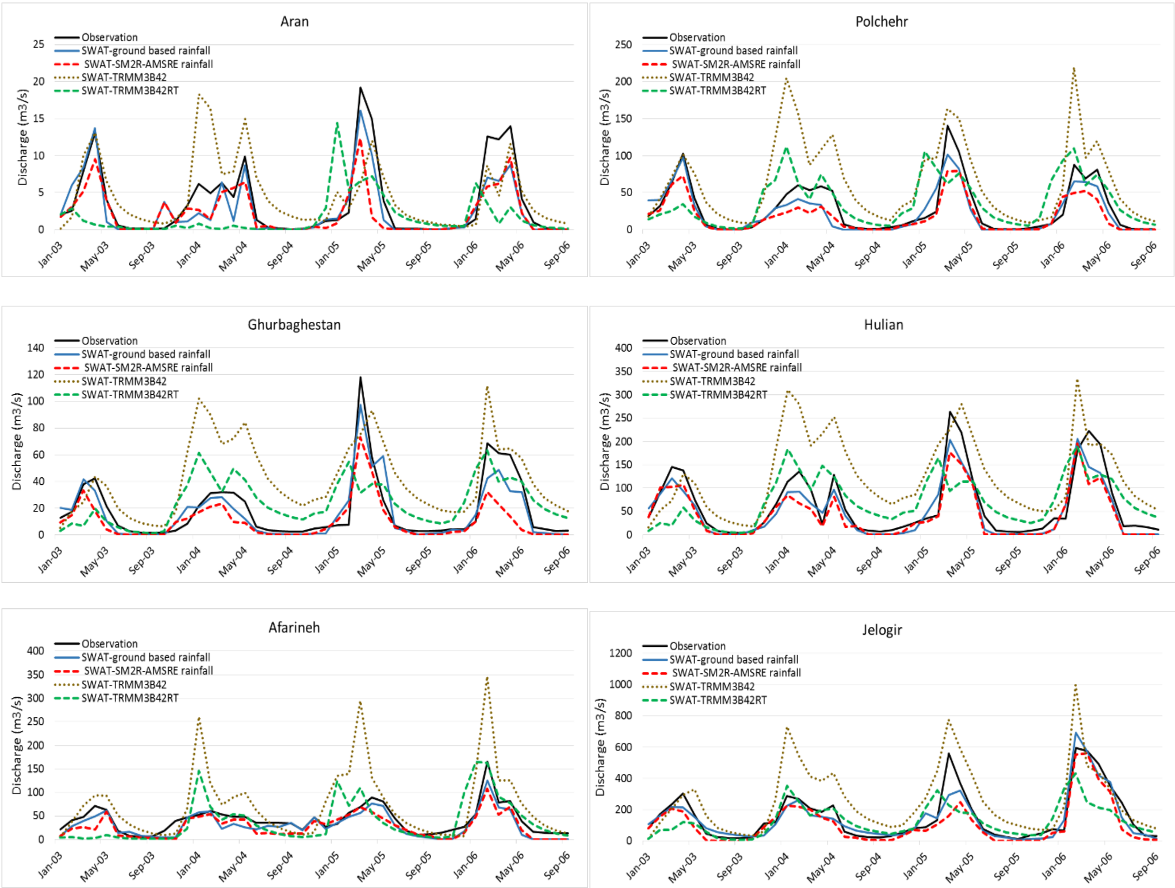

Figure 7. Observed and SWAT- simulated monthly streamflow for the 6 KRB gauge stations obtained using (1) ground-based, (2) satellite-based rainfall SM2R-AMSRE, and the two direct satellite-estimated (3) TRMM-3B42 and (4) TRMM-3B42RT rainfall products.

The statistics of the SWAT-runoff results obtained with the two TRMM-products, 3B42 and 3B42RT, are listed in Table 8 and may be compared with those acquired when using ground-based and SM2R-AMSRE rainfall in Table 7. Thus, one notices that since SM2R-AMSRE rainfall has already been shown to be more precise than that of the two TMPA- products, it is of no surprise that the SWAT- runoff simulated using the former as input is also better than those of the latter. Regarding the two TMPA- SWAT- variants, that with 3B42 satellite rainfall shows overall better results in terms of R^2, but with higher Bias and RMSE than the one using 3B42RT rainfall. Relative bias on the monthly basis varies between -5.87 and -0.31 for TMPA-3B42, and -2.9 and 0.53 for TMPA-3B42RT rainfall.

Table 8. Performance measures for SWAT-predicted runoff using the two TRMM-TMPA- predicted rainfall.

Station	TMPA- 3B42 satellite rainfall					TMPA- 3B42RT satellite rainfall				
	R^2	RMSE (m^3/s)	RRMSE	NSE	Bias	R^2	RMSE (m^3/s)	RRMSE	NSE	Bias
Aran	0.47	3.97	1.13	0.35	-1.10	0.12	5.15	1.46	0.11	1.85
Polchehr	0.62	52.1	1.84	0.33	-37.1	0.33	31.9	1.12	0.12	-9.30
Ghurbaghestan	0.39	132	7.18	-0.09	108.9	0.23	69.9	3.80	-0.07	-54.1
Hulian	0.48	89.9	1.43	-0.16	-64.2	0.29	60.4	0.96	0.23	-9.44
Afarineh	0.62	63.3	1.56	-0.37	-31.7	0.37	36.2	0.89	-0.54	3.25
Jelogir	0.70	159	1.03	0.03	-103	0.47	118	0.77	0.44	25.89

4. Conclusions

Preprints (www.preprints.org) | NOT PEER-REVIEWED | Posted: 31 December 2018 doi:10.20944/preprints201812.0361.v1

Peer-reviewed version available at Water 2019, 11, 594; doi:10.3390/w11030594

The estimation of river discharge in poorly gauged basin is fundamental for flood risk mitigation and water resources management. Among the different hydrological variables that have impact on water discharge, rainfall is considered as the most important one. The recently developed SM2RAIN algorithm [51] can be used for rainfall estimation from satellite soil moisture observations and it has been successfully applied to many regions for rainfall estimation (e.g., [55]). However, the use of SM2RAIN-derived rainfall for river discharge estimation has been less explored [18,56,57].

In this study, the SM2RAIN algorithm is successfully applied in the semi-arid Karkheh river basin in Iran to convert AMSR-E satellite SM product to daily rainfall at 10 meteorological stations. Good correlations R, ranging from 0.58 to 0.88, between the satellite-derived and the observed ground-based rainfall are obtained. Then the SM2R-AMSRE rainfall are used as input into a previously calibrated-SWAT model to estimate the monthly river discharge at 6 gauging stations in the basin. Good agreement with the observations, with R^2- values ranging between 0.72 and 0.87, are obtained, which is slightly less than the range obtained with the SWAT model using ground-based rainfall as input ($R^2 \sim 0.83$-0.89). Indeed, there is a small but systematic underestimation of the SWAT-SM2R-AMSRE simulated streamflow, owing to the fact that the SM2R-AMSRE rainfall estimated with the SM2RAIN algorithm is also smaller than the ground-based one, which in turn, is due to the possibility of saturation of the satellite-retrieved soil moisture level. In spite of these restrictions, the overall good performance of the SM2RAIN algorithm for rainfall and river discharge (via SWAT) estimation in the Karkheh basin here opens new possibilities for discharge estimation throughout Iran, also by using more recent and more versatile satellite SM products, as started to be investigated by [58].

Furthermore, the two well-known TRMM-satellite-based rainfall products, TMPA-3B42 and TMPA-3B42RT are assessed at the KRB climate stations and compared with both ground-based and the SM2E-AMSRE predictions. The results show that these TMPA-products predict the observed rainfall consistently less accurately than the SM2RAIN model. Similarly to SWAT- SM2R-AMSRE-simulated streamflow, the two TMPA-products are used as input into the previously calibrated-SWAT model. Expectedly, these SWAT-TMPA versions simulate the monthly runoff also less well than the SWAT- SM2R-AMSRE version, indicating again that using SM2R-AMSRE rainfall data in a hydrological model is a viable approach in basins with limited ground-based rainfall data.

.

Author Contributions: Conceptualization, Majid Fereidoon; Formal analysis, Majid Fereidoon and Luca Brocca; Funding acquisition, Manfred Koch; Methodology, Majid Fereidoon; Software, Majid Fereidoon; Supervision, Manfred Koch and Luca Brocca; Validation, Majid Fereidoon; Writing – original draft, Majid Fereidoon; Writing – review & editing, Manfred Koch and Luca Brocca.

Funding: This work was supported by Deutscher AkademischerAustausch Dienst (DAAD) via the PhD/grant ref. no: 91549378.

Conflicts of Interest: The authors declare no conflict of interest.

References

1. Remesan, R.; Shamim, M.A.; Han, D.; Mathew, J. Runoff prediction using an integrated hybrid modelling scheme. *Journal of Hydrology* **2009**, *372*, 48–60.
2. Stefanidis, S.; Stathis, D. Assessment of flood hazard based on natural and anthropogenic factors using analytic hierarchy process (AHP). *Nat Hazards* **2013**, *68*, 569–585.
3. Wang, Z.; Lai, C.; Chen, X.; Yang, B.; Zhao, S.; Bai, X. Flood hazard risk assessment model based on random forest. *Journal of Hydrology* **2015**, *527*, 1130–1141.
4. Li, Y.; Ryu, D.; Western, A.W.; Wang, Q.J. Assimilation of stream discharge for flood forecasting: Updating a semidistributed model with an integrated data assimilation scheme. *Water Resour. Res.* **2015**, *51*, 3238–3258.
5. Li, H.; Zhang, Y.; Vaze, J.; Wang, B. Separating effects of vegetation change and climate variability using hydrological modelling and sensitivity-based approaches. *Journal of Hydrology* **2012**, *420-421*, 403–418.
6. Arnold, J.G.; Srinivasan, R.; Muttiah, R.S.; Williams, J.R. LARGE AREA HYDROLOGIC MODELING AND ASSESSMENT PART I: MODEL DEVELOPMENT. *J Am Water Resources Assoc* **1998**, *34*, 73–89.

 doi:10.20944/preprints201812.0361.v1

Peer-reviewed version available at *Water* **2019**, *11*, 594; doi:10.3390/w11030594

7. Gassman, P.W.; Reyes, M.R.; Green, C.H.; Arnold, J.G. The Soil and Water Assessment Tool: Historical Development, Applications, and Future Research Directions. *Transactions of the ASABE* **2007**, *50*, 1211–1250.
8. Bárdossy, A. Calibration of hydrological model parameters for ungauged catchments. *Hydrol. Earth Syst. Sci.* **2007**, *11*, 703–710.
9. Ercan, M.B.; Goodall, J.L.; Castronova, A.M.; Humphrey, M.; Beekwilder, N. Calibration of SWAT models using the cloud. *Environmental Modelling & Software* **2014**, *62*, 188–196.
10. Masih, I.; Maskey, S.; Uhlenbrook, S.; Smakhtin, V. Assessing the Impact of Areal Precipitation Input on Streamflow Simulations Using the SWAT Model1. *J Am Water Resources Assoc* **2011**, *47*, 179–195.
11. Strauch, M.; Bernhofer, C.; Koide, S.; Volk, M.; Lorz, C.; Makeschin, F. Using precipitation data ensemble for uncertainty analysis in SWAT streamflow simulation. *Journal of Hydrology* **2012**, *414-415*, 413–424.
12. Voisin, N.; Wood, A.W.; Lettenmaier, D.P. Evaluation of Precipitation Products for Global Hydrological Prediction. *J. Hydrometeor* **2008**, *9*, 388–407.
13. Kidd, C.; Bauer, P.; Turk, J.; Huffman, G.J.; Joyce, R.; Hsu, K.-L.; Braithwaite, D. Intercomparison of High-Resolution Precipitation Products over Northwest Europe. *J. Hydrometeor* **2012**, *13*, 67–83.
14. Bitew, M.M.; Gebremichael, M. Evaluation of satellite rainfall products through hydrologic simulation in a fully distributed hydrologic model. *Water Resour. Res.* **2011**, *47*, 45.
15. Casse, C.; Gosset, M.; Peugeot, C.; Pedinotti, V.; Boone, A.; Tanimoun, B.A.; Decharme, B. Potential of satellite rainfall products to predict Niger River flood events in Niamey. *Atmospheric Research* **2015**, *163*, 162–176.
16. Wang, S.; Liu, S.; Mo, X.; Peng, B.; Qiu, J.; Li, M.; Liu, C.; Wang, Z.; Bauer-Gottwein, P. Evaluation of Remotely Sensed Precipitation and Its Performance for Streamflow Simulations in Basins of the Southeast Tibetan Plateau. *J. Hydrometeor* **2015**, *16*, 2577–2594.
17. Pakoksung, K.; Takagi, M. Effect of satellite based rainfall products on river basin responses of runoff simulation on flood event. *Model. Earth Syst. Environ.* **2016**, *2*, 2024.
18. Ciabatta, L.; Brocca, L.; Massari, C.; Moramarco, T.; Gabellani, S.; Puca, S.; Wagner, W. Rainfall-runoff modelling by using SM2RAIN-derived and state-of-the-art satellite rainfall products over Italy. *International Journal of Applied Earth Observation and Geoinformation* **2016**, *48*, 163–173
19. Yoshimoto, S.; Amarnath, G. Applications of Satellite-Based Rainfall Estimates in Flood Inundation Modeling—A Case Study in Mundeni Aru River Basin, Sri Lanka. *Remote Sensing* **2017**, *9*, 998.
20. Stisen, S.; Sandholt, I. Evaluation of remote-sensing-based rainfall products through predictive capability in hydrological runoff modelling. *Hydrol. Process.* **2010**, *24*, 879–891.
21. Thiemig, V.; Rojas, R.; Zambrano-Bigiarini, M.; Roo, A. de. Hydrological evaluation of satellite-based rainfall estimates over the Volta and Baro-Akobo Basin. *Journal of Hydrology* **2013**, *499*, 324–338.
22. Huffman, G.J.; Bolvin, D.T.; Nelkin, E.J.; Wolff, D.B.; Adler, R.F.; Gu, G.; Hong, Y.; Bowman, K.P.; Stocker, E.F. The TRMM Multisatellite Precipitation Analysis (TMPA): Quasi-Global, Multiyear, Combined-Sensor Precipitation Estimates at Fine Scales. *J. Hydrometeor* **2007**, *8*, 38–55.
23. Gourley, J.J.; Hong, Y.; Flamig, Z.L.; Wang, J.; Vergara, H.; Anagnostou, E.N. Hydrologic Evaluation of Rainfall Estimates from Radar, Satellite, Gauge, and Combinations on Ft. Cobb Basin, Oklahoma. *J. Hydrometeor* **2011**, *12*, 973–988.
24. Bitew, M.M.; Gebremichael, M.; Ghebremichael, L.T.; Bayissa, Y.A. Evaluation of High-Resolution Satellite Rainfall Products through Streamflow Simulation in a Hydrological Modeling of a Small Mountainous Watershed in Ethiopia. *J. Hydrometeor* **2012**, *13*, 338–350.
25. Dinku, T.; Ceccato, P.; Grover-Kopec, E.; Lemma, M.; Connor, S.J.; Ropelewski, C.F. Validation of satellite rainfall products over East Africa's complex topography. *International Journal of Remote Sensing* **2007**, *28*, 1503–1526.
26. Brocca, L.; Moramarco, T.; Melone, F.; Wagner, W. A new method for rainfall estimation through soil moisture observations. *Geophys. Res. Lett.* **2013**, *40*, 853–858.
27. Brocca, L.; Massari, C.; Ciabatta, L.; Moramarco, T.; Penna, D.; Zuecco, G.; Pianezzola, L.; Borga, M.; Matgen, P.; Martínez-Fernández, J. Rainfall estimation from in situ soil moisture observations at several sites in Europe: an evaluation of the SM2RAIN algorithm. *Journal of Hydrology and Hydromechanics* **2015**, *63*, 201–209.
28. Rahmani, A.; Golian, S.; Brocca, L. Multiyear monitoring of soil moisture over Iran through satellite and reanalysis soil moisture products. *International Journal of Applied Earth Observation and Geoinformation* **2016**, *48*, 85–95.

29. Sahoo, A.K.; Houser, P.R.; Ferguson, C.; Wood, E.F.; Dirmeyer, P.A.; Kafatos, M. Evaluation of AMSR-E soil moisture results using the in-situ data over the Little River Experimental Watershed, Georgia. *Remote Sensing of Environment* **2008**, *112*, 3142–3152.
30. Fereidoon, M.; Koch, M. Rainfall Prediction with AMSR–E Soil Moisture Products Using SM2RAIN and Nonlinear Autoregressive Networks with Exogenous Input (NARX) for Poorly Gauged Basins: Application to the Karkheh River Basin, Iran. *Water* **2018**, *10*, 964.
31. Martinez, G.; Brocca, L.; Gerke, H.H.; Pachepsky, Y.A. Soil Variability and Biogeochemical Fluxes: Toward a Better Understanding of Soil Processes at the Land Surface. *Vadose Zone Journal* **2017**, *16*, 0.
32. Albergel, C.; Dorigo, W.; Balsamo, G.; Muñoz-Sabater, J.; Rosnay, P. de; Isaksen, L.; Brocca, L.; Jeu, R. de; Wagner, W. Monitoring multi-decadal satellite earth observation of soil moisture products through land surface reanalyses. *Remote Sensing of Environment* **2013**, *138*, 77–89.
33. Kerr, Y.H.; Waldteufel, P.; Wigneron, J.-P.; Martinuzzi, J.; Font, J.; Berger, M. Soil moisture retrieval from space: the Soil Moisture and Ocean Salinity (SMOS) mission. *IEEE Trans. Geosci. Remote Sensing* **2001**, *39*, 1729–1735.
34. Entekhabi, D.; Yueh, S.; O'Neill, P.E.; Kellogg, K.H.; Allen, A.; Bindlish, R.; Brown, M.; Chan, S.; Colliander, A.; Crow, W.T. *SMAP Handbook–Soil Moisture Active Passive: Mapping Soil Moisture and Freeze/Thaw From Space;* Jet Propulsion Laboratory: Pasadena, CA, USA, 2014.
35. Gruhier, C.; Rosnay, P. de; Hasenauer, S.; Holmes, T.; Jeu, R. de; Kerr, Y.; Mougin, E.; Njoku, E.; Timouk, F.; Wagner, W.; *et al.* Soil moisture active and passive microwave products: intercomparison and evaluation over a Sahelian site. *Hydrol. Earth Syst. Sci.* **2010**, *14*, 141–156.
36. Santi, E.; Paloscia, S.; Pettinato, S.; Brocca, L.; Ciabatta, L. Robust Assessment of an Operational Algorithm for the Retrieval of Soil Moisture From AMSR-E Data in Central Italy. *IEEE J. Sel. Top. Appl. Earth Observations Remote Sensing* **2016**, *9*, 2478–2492.
37. Njoku, E.G.; Jackson, T.J.; Lakshmi, V.; Chan, T.K.; Nghiem, S.V. Soil moisture retrieval from AMSR-E. *IEEE Trans. Geosci. Remote Sensing* **2003**, *41*, 215–229.
38. Li, Q.; Zhong, R.; Huang, J.; Gong, H. Comparison of two retrieval methods with combined passive and active microwave remote sensing observations for soil moisture. *Mathematical and Computer Modelling* **2011**, *54*, 1181–1193.
39. Kim, H.; Parinussa, R.; Konings, A.G.; Wagner, W.; Cosh, M.H.; Lakshmi, V.; Zohaib, M.; Choi, M. Global-scale assessment and combination of SMAP with ASCAT (active) and AMSR2 (passive) soil moisture products. *Remote Sensing of Environment* **2018**, *204*, 260–275.
40. Brocca, L.; Hasenauer, S.; Lacava, T.; Melone, F.; Moramarco, T.; Wagner, W.; Dorigo, W.; Matgen, P.; Martínez-Fernández, J.; Llorens, P.; *et al.* Soil moisture estimation through ASCAT and AMSR-E sensors: An intercomparison and validation study across Europe. *Remote Sensing of Environment* **2011**, *115*, 3390–3408.
41. Babaeian, E.; Homaee, M.; Montzka, C.; Vereecken, H.; Norouzi, A.A.; van Genuchten, M.T. Soil moisture prediction of bare soil profiles using diffuse spectral reflectance information and vadose zone flow modeling. *Remote Sensing of Environment* **2016**, *187*, 218–229.
42. Al-Yaari, A.; Wigneron, J.-P.; Ducharne, A.; Kerr, Y.H.; Wagner, W.; Lannoy, G. de; Reichle, R.; Al Bitar, A.; Dorigo, W.; Richaume, P.; *et al.* Global-scale comparison of passive (SMOS) and active (ASCAT) satellite based microwave soil moisture retrievals with soil moisture simulations (MERRA-Land). *Remote Sensing of Environment* **2014**, *152*, 614–626.
43. Abbaspour, K.C.; Johnson, C.A.; van Genuchten, M.T. Estimating Uncertain Flow and Transport Parameters Using a Sequential Uncertainty Fitting Procedure. *Vadose Zone Journal* **2004**, *3*, 1340–1352.
44. Muthuwatta, L.P.; Ahmad, M.-u.-D.; Bos, M.G.; Rientjes, T.H.M. Assessment of Water Availability and Consumption in the Karkheh River Basin, Iran—Using Remote Sensing and Geo-statistics. *Water Resour Manage* **2010**, *24*, 459–484.
45. Jamali, S.; Abrishamchi, A.; Marino, M.A.; Abbasnia, A. Climate change impact assessment on hydrology of Karkheh Basin, Iran. *Proceedings of the Institution of Civil Engineers - Water Management* **2013**, *166*, 93–104.
46. Fereidoon, M.; Koch, M. SWAT-modeling of the effects of the construction of a dam on streamflow in the Karkheh basin, Iran. *Journal of Thai Interdisciplinary Research* **2017**, *12*, 79–86.
47. Jackson, T.J.; Cosh, M.H.; Bindlish, R.; Starks, P.J.; Bosch, D.D.; Seyfried, M.; Goodrich, D.C.; Moran, M.S.; Du, J. Validation of Advanced Microwave Scanning Radiometer Soil Moisture Products. *IEEE Trans. Geosci. Remote Sensing* **2010**, *48*, 4256–4272.

48. Varanou, E.; Gkouvatsou, E.; Baltas, E.; Mimikou, M. Quantity and Quality Integrated Catchment Modeling under Climate Change with use of Soil and Water Assessment Tool Model. *Journal of Hydrologic Engineering* **2002**, *7*, 228–244.
49. Kundu, S.; Khare, D.; Mondal, A. Individual and combined impacts of future climate and land use changes on the water balance. *Ecological Engineering* **2017**, *105*, 42–57.
50. Fereidoon, M.; Koch, M. SWAT-MODSIM-PSO optimization of multi-crop planning in the Karkheh River Basin, Iran, under the impacts of climate change. *The Science of the total environment* **2018**, *630*, 502–516.
51. Brocca, L.; Ciabatta, L.; Massari, C.; Moramarco, T.; Hahn, S.; Hasenauer, S.; Kidd, R.; Dorigo, W.; Wagner, W.; Levizzani, V. Soil as a natural rain gauge: Estimating global rainfall from satellite soil moisture data. *J. Geophys. Res. Atmos.* **2014**, *119*, 5128–5141.
52. Doorenbos, J.; Pruitt, W.O. Background and Development of Methods to Predict Reference Crop Evapotranspiration (ETo); Appendix II in FAO-ID-24; FAO: Rome, Italy, 1977; pp. 108–119.
53. Schmalz, B.; Fohrer, N. Comparing model sensitivities of different landscapes using the ecohydrological SWAT model. *Adv. Geosci.* **2009**, *21*, 91–98.
54. Crow, W.T.; Berg, A.A.; Cosh, M.H.; Loew, A.; Mohanty, B.P.; Panciera, R.; Rosnay, P. de; Ryu, D.; Walker, J.P. Upscaling sparse ground-based soil moisture observations for the validation of coarse-resolution satellite soil moisture products. *Rev. Geophys.* **2012**, *50*, 3675.
55. Ciabatta, L.; Massari, C.; Brocca, L.; Gruber, A.; Reimer, C.; Hahn, S.; Paulik, C.; Dorigo, W.; Kidd, R.; Wagner, W. SM2RAIN-CCI: a new global long-term rainfall data set derived from ESA CCI soil moisture. *Earth Syst. Sci. Data* **2018**, *10*, 267–280.
56. Abera, W.; Formetta, G.; Brocca, L.; Rigon, R. Modeling the water budget of the Upper Blue Nile basin using the JGrass-NewAge model system and satellite data. *Hydrol. Earth Syst. Sci.* **2017**, *21*, 3145–3165.
57. Massari, C.; Camici, S.; Ciabatta, L.; Brocca, L. Exploiting Satellite-Based Surface Soil Moisture for Flood Forecasting in the Mediterranean Area: State Update Versus Rainfall Correction. *Remote Sensing* **2018**, *10*, 292.
58. Tarpanelli, A.; Massari, C.; Ciabatta, L.; Filippucci, P.; Amarnath, G.; Brocca, L. Exploiting a constellation of satellite soil moisture sensors for accurate rainfall estimation. *Advances in Water Resources* **2017**, *108*, 249–255.